

To appear in *ApJ Letters*

The $z = 1.6748$ C I Absorber Toward PKS 1756+237

Katherine C. Roth^{1,2,3} and James M. Bauer²

Institute for Astronomy, University of Hawaii, 2680 Woodlawn Drive, Honolulu, HI 96825

ABSTRACT

We report the detection of the $\lambda 1560$ and $\lambda 1657$ ground-state C I absorption features in the $z_{\text{abs}} = 1.6748$ system toward the QSO PKS 1756+237. We find no associated C I* lines with a resulting 3σ excitation temperature upper-limit of $T_{\text{ex}} \leq 8.54 (+0.65, -0.56)$ K, which is consistent with the predicted CMBR temperature of $T_{\text{CMBR}} = 7.291$ K. Because the redshifted CMBR populates the $J = 1$ level and leaves little room for additional local excitation through either collisions or UV pumping, our data place 2–3 times more stringent limits on particle densities and UV fields than existing *Copernicus* observations of similar column density sightlines in the Milky Way. We also detect several Ni II lines and the weak Fe II $\lambda 1611$ line. From the Ni/Fe column density ratio we find evidence for dust at a dust-to-metals ratio similar to that seen toward warm Galactic disk clouds. Based on these findings and supported by our Ly α spectrum we propose to reclassify this system as a damped Ly α absorber.

Subject headings: cosmic microwave background — quasars: absorption lines — quasars: individual (PKS 1756+237) — ISM: abundances — dust

1. Introduction

Absorption spectra of QSOs sample the distribution and physical state of intervening gaseous material in the early universe. Damped Ly α systems ($\log N(\text{HI}) \gtrsim 20.3 \text{ cm}^{-2}$) are particularly important since they are believed to originate within young galaxies or galaxy building blocks. The

¹Hubble Fellow

²Visiting Astronomer, W.M. Keck Observatory, operated as a scientific partnership among the California Institute of Technology, the University of California and NASA. WMKO was made possible by the generous financial support of the W.M. Keck Foundation.

³current address: Dept. of Physics & Astronomy, Johns Hopkins University, 3400 N. Charles St., Baltimore, MD 21218 — e-mail: kroth@pha.jhu.edu

simple ionization state and high column densities within these systems enable the determination of accurate abundances for many species. Metallicities are commonly based on Zn II and S II measurements, while Fe-peak elements, eg. Cr II, Fe II, and Ni II, are used to infer depletion estimates of dust grain formation. Abundances of α -process elements, eg. Si II, Mn II, and Ti II, may reflect the importance of high-mass stars to the enrichment of the interstellar medium (ISM) within the absorbers. The excitation of C I fine-structure levels depends upon the gas pressure. Also, redshifted Cosmic Microwave Background Radiation (CMBR) photons excite C I more efficiently than the present-day CMBR due to the predicted temperature dependence on redshift, $T = T_{\text{CMBR}}(1 + z)$. Therefore, measurements of C I excitation in damped Ly α systems can yield sensitive upper-limits on the temperature of the CMBR in the past, testing the fundamental prediction of simple big bang cosmologies that the universe cools as it expands. Neutral species like C I are associated in the Milky Way ISM primarily with dense, molecule-rich lines of sight. Only three high-redshift C I absorbers are known (Ge et al. 1997, Songaila et al. 1994, Meyer et al. 1986, Blades et al. 1985, Blades et al. 1982), consistent with the apparent lack of molecules in many damped Ly α systems. In this Letter we report the unexpected detection of C I absorption at $z = 1.6748$ toward the QSO PKS 1756+237.

2. Observations and Analysis

PKS 1756+237 ($m_V = 18.0$, $z_{\text{em}} = 1.721$) was observed May 30 and 31, 1997 using the W. M. Keck Observatory I 10-m High Resolution Echelle Spectrometer (HIRES, Vogt et al. 1994) for two hours. The signal-to-noise ratio varies from ~ 5 at the blue end to $\gtrsim 25$ at longer wavelengths. Two slightly offset grating tilt angles yielded complete spectral coverage from 3190 – 5055 Å with a resolution of 35,000 (FWHM = 8.5 km s $^{-1}$). Full details of the spectra extraction and reduction procedures, along with a complete analysis of all the observed spectral features, will be presented in our companion paper (Roth et al. 1999). Among the surprises found in the $z = 1.6748$ absorption system are several Ni II lines, Fe II $\lambda 1611$, and C I $\lambda\lambda 1657, 1560$. None of these were expected to be present because of the low H I column density in this absorber, $\log N(\text{HI}) \sim 19.5$ (Turnshek et al. 1979). Figure 1 shows these lines plotted versus heliocentric corrected rest vacuum velocity along with C II* $\lambda 1336$ and Si II $\lambda 1527$. We have examined the entire spectrum for other absorption systems which may confuse individual features in the $z = 1.6748$ absorber. The only possibility is a system $z = 1.7337$, probably associated with the QSO, which could be contaminating our C I $\lambda 1560$ line profile with Si II $\lambda 1527$ absorption. However, we discount it as insignificant because this absorber has a high ionization state and the corresponding C II $\lambda 1335$ line, expected to be much stronger than Si II $\lambda 1527$, is quite weak (≈ 20 mÅ).

In this Letter we largely restrict our analysis to the weak features in Figure 1 which trace the highest column density neutral cloud harboring C I. Equivalent widths (W_λ) are measured by direct integration across the line profiles. Statistical W_λ errors are estimated from the signal-to-noise ratio in the adjacent continuum (Jenkins 1973). To account for continuum placement uncertainties

we inflate the errors $\sigma(W_\lambda)$ to equal 150% of the formal statistical values. The resulting rest equivalent width measurements and column densities resulting from a linear curve-of-growth (N_{linear}) are given in Table 1. The good N_{linear} agreement among different absorption lines from the same species suggests that most of these weak features are unsaturated. Therefore our column density measurements will be largely insensitive to the adopted model line profile. Our three-component Voigt profile absorption model is given in Table 2. We have convolved this model with a Gaussian instrumental b -value of 5.1 km s^{-1} to produce the superimposed profiles presented in Figure 1. The total model column density in all three velocity components is given in the last column of Table 1. Note that the C I absorption, which presumably arises from the densest material, is present only in the central narrow velocity component.

3. Abundances and Depletions

Fe II, Ni II, and Si II are dominant ionization stages in neutral H I material and thus measure gas-phase abundances. Fe and Ni are both Fe-peak elements and deplete readily onto dust grains in the Milky Way ISM. Si is formed via the α -process and is much less susceptible to dust, but its abundance relative to Fe and Ni may depend on star formation history. For these reasons, the interpretation of relative abundance ratios is complicated (eg. Vladilo 1998, Pettini et al. 1997a, Lu et al. 1996). The cosmic abundances for Si, Fe and Ni have relative values of $1.00 : 0.91 : 0.050$ (Anders & Grevesse 1989) while our observed relative abundances (Table 1) are $1.00 : 1.16 : 0.031$. The observed 2σ enhancement of Fe over Si is probably not significant since the Si II $\lambda 1808$ feature is 75% deep and therefore possibly saturated. However, the observed deficit of Ni with respect to Fe is more likely to be real. The Fe abundance arises from the very weak Fe II $\lambda 1611$ feature which is unaffected by saturation. Therefore the Fe II column density uncertainty is simply the 14% equivalent width measurement error. We estimate the Ni II column density 1σ uncertainty to be $\pm 3.6\%$ from a weighted average of the six linear curve-of-growth 1σ values. This leads to an observed Ni/Fe abundance ratio of 0.027 ± 0.004 , significantly below the cosmic Ni/Fe value of 0.055. Since both Fe and Ni are Fe-peak elements, this observed deviation in the relative gas-phase abundances from the cosmic value is likely due to depletion onto grains. Diffuse clouds in the Milky Way ISM come in roughly three categories with different physical conditions and dust depletion properties. In order of increasing temperature and decreasing density, these are cool disk clouds, warm disk clouds and halo clouds with gas-phase Ni/Fe values of $0.012 - 0.035$, $0.028 - 0.035$, and $0.026 - 0.046$, respectively (Sembach & Savage 1996). Our measured Ni/Fe abundance ratio is completely consistent with galactic dust depletion, perhaps suggestive of warm disk gas. Unfortunately, our data do not extend to long enough wavelengths to cover Zn II and Cr II. These lines should be easily detectable, and the relative abundance ratios Ni/Zn, Fe/Zn or Cr/Zn show a more pronounced variation with ISM environment because Zn is observed to deplete very little, if at all, onto dust grains (eg. Pettini et al. 1997b, Roth & Blades 1995, Sembach et al. 1995).

4. Carbon I Excitation

We report the very surprising detection of C I ground-state absorption in the $z = 1.6748$ gas cloud (Figure 2, Table 1). Since the lines are somewhat saturated, we have applied a $b = 2.5$ km/s Gaussian curve-of-growth to our equivalent width measurement errors to estimate the uncertainty in our model column density value (Table 2), yielding $N(\text{CI}) = 1.41(+0.30, -0.25) \times 10^{13}$ cm $^{-2}$. We do not detect any C I* excited-state lines. While in the Galactic ISM the dominant C I excitation mechanism is neutral particle collisions, at high redshift the CMBR will make a non-negligible contribution to the population of the $J = 1$ level. The amount of pumping is given by the Boltzmann equation:

$$T_{\text{CMBR}}(1+z) = \frac{h\nu_{0 \rightarrow 1}}{k_B} \left\{ \ln \left(\frac{3n_{J=0}}{n_{J=1}} \right) \right\}^{-1} \quad (1)$$

where $\nu_{0 \rightarrow 1}$ is the frequency of the energy separation between the ground and first-excited states, $(h\nu_{0 \rightarrow 1}/k_B) = 23.595$ K (Nussbaumer & Rusca 1979), and the present-day CMBR temperature $T_{\text{CMBR}} = 2.726$ K (Mather et al. 1994). Replacing the number density ratio $n_{J=1}/n_{J=0}$ by the observable quantity $N_{J=1}/N_{J=0}$ in Equation 1, we predict an excited-state column density of $N(\text{CI}^*) = 1.67(+0.35, -0.30) \times 10^{12}$ cm $^{-2}$. On Figure 2 we superimpose the predicted C I* absorption profiles. As can be seen, the detection limit of our data is just above the C I* line strengths produced by the redshifted $T = 7.291$ K CMBR.

To improve our C I* detection limit, we have shifted the observed data points to a common velocity scale for each of the four excited-state features (for the C I* $\lambda 1561$ doublet we use an f -value weighted average line center). This average C I* spectrum is shown in the inset to Figure 2, where we have superimposed the predicted C I* profile produced using the same stacking method. The rms error of the inset stacked spectral region ($S/N = 45$) corresponds to an equivalent width error over nine pixels of 0.75 mÅ. We inflate this σ_{W_λ} by 50% for the same reason as before and adopt a 1σ uncertainty in the stacked C I* equivalent width of 1.1 mÅ. The stacked C I* profile has an equivalent width of 2.1 mÅ, which is consistent with no local excitation of the C I fine-structure levels above CMBR pumping at the 2σ level. However, since inspection of the stacked C I* spectrum suggests that some absorption might be present, although at somewhat less than our 2σ level, we have elected to adopt a 3σ detection upper-limit for this stacked C I* feature of $W_\lambda(\text{CI}^*) \leq 3.3$ mÅ, which implies a 3σ C I* column density upper-limit of $N(\text{CI}^*) \leq 2.67 \times 10^{12}$ cm $^{-2}$. This leads to a 3σ upper-limit on the C I excitation temperature in the $z = 1.6748$ absorber toward PKS 1756+237 of $T_{\text{ex}} \leq 8.54(+0.65, -0.56)$ K. The stacked profile for this 3σ detection limit is shown by the dashed line in the inset to Figure 2.

In addition to measuring the CMBR temperature, our C I fine-structure population measurement allows us to determine the physical conditions within the absorbing gas cloud. For collisional excitation by hydrogen atoms, we employ the rate coefficients reported by Launay & Rueeff 1977. For UV pumping, we solve the detailed balance population equations for the 200 strongest C I UV lines (de Boer & Morton 1974, Jenkins et al. 1983, Morton 1991, Zsargo et al.

1997) and measure the UV field in units of the WJ1 average interstellar radiation field (Morton 1975 [Table 9], de Boer et al. 1973, Witt & Johnson 1973). In the absence of CMBR pumping and collisional excitation, we find a 3σ upper-limit on the UV field within the $z = 1.6748$ absorber of $\leq 14.3 (+3.2, -2.6)$ times the Galactic UV radiation field. Alternatively, if collisions alone populate the $J = 1$ level and the gas kinetic temperature is 10 K, typical of cool disk clouds, the hydrogen atom density is (3σ upper-limit) $n_{\text{H}}^{10\text{K}} \leq 950 (+1079, -369) \text{ cm}^{-3}$. The C I collisional excitation rate is very sensitive at low temperatures. For example, at a slightly higher temperature (15 K) the density limits are reduced significantly ($n_{\text{H}}^{15\text{K}} \leq 191 (+64, -44) \text{ cm}^{-3}$). At kinetic temperatures similar to less dense clouds or halo clouds (100 or 1000 K) the upper-limits are further decreased to $n_{\text{H}}^{100\text{K}} \leq 25.1 (+5.8, -4.6)$ and $n_{\text{H}}^{1000\text{K}} \leq 10.6 (+2.4, -1.9) \text{ cm}^{-3}$.

These limits become more interesting when one includes the considerable contribution to C I* excitation by the high redshift CMBR. As a result, observations of C I fine-structure lines in QSO absorbers can yield far more sensitive probes of the physical conditions within distant gas clouds than similar observations within the Milky Way can provide. For example, if we assume the CMBR temperature at $z = 1.6748$ is given by the predicted big bang value of 7.291 K, we find that our UV field and hydrogen atom density upper-limits are substantially lower. With CMBR pumping, the ambient UV field must be less than (3σ) 5.6 ($+3.3, -2.6$) Galactic fields, $n_{\text{H}}^{10\text{K}} \leq 371 (+652, -224) \text{ cm}^{-3}$, $n_{\text{H}}^{15\text{K}} \leq 75 (+54, -37) \text{ cm}^{-3}$, $n_{\text{H}}^{100\text{K}} \leq 9.8 (+5.8, -4.6) \text{ cm}^{-3}$, and $n_{\text{H}}^{1000\text{K}} \leq 4.1 (+2.4, -1.9) \text{ cm}^{-3}$.

In a survey of 27 Galactic stars using the *Copernicus* satellite, Jenkins et al. 1983 did not report an excitation temperature lower than 40 K and excited-state lines were detected in 23 lines of sight. However, excitation temperatures were not determinable for nearly 25% of their sample, and all four of the sightlines lacking C I* absorption had $N(\text{CI})$ values that were comparable to or below that found in the $z = 1.6748$ absorber. Because of the redshifted CMBR, our limits on the physical conditions within the $z = 1.6748$ absorber are 2–3 times lower than the values in these four Milky Way sightlines. It is perhaps too early to tell whether high-redshift C I absorbers are similar to Milky Way low column density sightlines, or if there is a deficit of high column density C I absorbers toward QSOs. The discovery of more high-redshift C I QSO systems will eventually answer the latter question, while higher quality C I spectra of the Milky Way ISM are required to address the former.

5. A Damped Ly α Absorber?

The presence of weak, singly-ionized metal lines and C I argue strongly that the $z = 1.6748$ absorber toward PKS 1756+237 has been erroneously classified as a moderately low column density system and we have assumed it is in fact damped. Our spectral data extend far enough into the blue to cover the H I absorption feature, and we have attempted to verify the validity of this claim. The Ly α line, smoothed and rebinned to 20% the resolution, is presented in Figure 3 with model Voigt profiles for the originally reported $\log N(\text{HI}) \sim 19.5$ (Turnshek et al. 1979) and

a damped Ly α absorber superimposed. The data are noisy, the Ly α absorption is located near the blue wing of the QSO Ly α emission ($z_{\text{em}} = 1.721$), and it extends across two echelle orders, all of which complicate the continuum placement. For these reasons, we do not claim a conclusive H I column density measurement. However, we believe there is sufficient evidence to reclassify this system as a damped Ly α absorber with ≈ 6 –10 times more neutral material than previously reported.

The authors wish to thank the staff at WMKO for their excellent technical assistance in executing the observations. KCR is grateful to Antoinette Songaila for her advice and support as faculty sponsor at the Institute for Astronomy, and to Ken Sembach for extremely helpful discussions and suggestions. JMB acknowledges and thanks Alan Stockton for his role as faculty contact during his AST699 Graduate Student Research Project. Funding for this work was provided in part by NASA through Hubble Fellowship grant #HF-01076.01-94A and grants #GO-05887.02-94A, #GO-05888.01-94A awarded by the Space Telescope Science Institute, which is operated by the Association of Universities for Research in Astronomy, Inc., for NASA under contract NAS5-26555.

REFERENCES

Anders, E., & Grevesse, N. 1989, *Geochim. Cosmochim. Acta*, 53, 197

Blades, J.C., Hunstead, R.W., Murdoch, H.S., & Pettini, M. 1982, *MNRAS*, 200, 1091

Blades, J.C., Hunstead, R.W., Murdoch, H.S., & Pettini, M. 1985, *ApJ*, 288, 580

Cardelli, J.A. & Savage, B.D. 1995, *ApJ*, 452, 275

de Boer, K.S., & Morton, D.C. 1974, *A&A*, 37, 305

de Boer, K.S., Koppenaal, K., & Pottasch, S.R. 1973 *A&A*, 28, 145; 29, 453

Ge, J., Bechtold, J., & Black, J.H. 1997, *ApJ*, 474, 67

Jenkins, E.B. 1973, *ApJ*, 181, 761

Jenkins, E.B., Jura, M., & Lowenstein, M. 1983, *ApJ*, 270, 88

Launay, J.M., & Reueff, E. 1977, *A&A*, 56, 289

Lu, L., Sargent, W.L.W., Barlow, T.A., Churchill, C.W., & Vogt, S.S. 1996, *ApJS*, 107, 475

Mather, J.C. et al. 1994, *ApJ*, 354, L37

Meyer, D.M., York, D.G., Black, J.H., Chaffee, F.H., Jr., & Foltz, C.B. 1986, *ApJ*, 308, 37L

Morton, D.C. 1975, *ApJ*, 197, 85

Morton, D.C. 1991, *ApJS*, 77, 119

Nussbaumer, H., & Rusca, C. 1979, *A&A*, 72, 129

Pettini, M., King, D.L., Smith, L.J., & Hunstead, R.W. 1997, *ApJ*, 478, 536 (Pettini et al. 1997a)

Pettini, M., Smith, L.J., King, D.L., & Hunstead, R.W. 1997, *ApJ*, 486, 665 (Pettini et al. 1997b)

Roth, K.C., Bauer, J.M., & Jim, K.T.C. 1999, in preparation

Roth, K.C., & Blades, J.C. 1995, *ApJ*, 445, L95

Sembach, K.R., & Savage, B.D. 1996, *ApJ*, 457, 211

Sembach, K.R., Steidel, C.C., Macke, R.J., & Meyer, D.M. 1995, *ApJ*, 445, L27

Songaila, A., Cowie, L.L., Vogt, S., Keane, M., Wolfe, A.M., Hu, E.M., Oren, A.L., Tytler, D.R., & Lanzetta, K.M. 1994, *Nature*, 371, 43

Turnshek, D.A., Weymann, R.J., & Williams, R.E. 1979, *ApJ*, 230, 330

Vladilo, G. 1998, *ApJ*, 493, 583

Vogt, S.S., Allen, S.L., Bigelow, B.C., Bresee, L., Brown, B., Cantrall, T., Conrad, A., Couture, M., Delaney, C., Epps, H.W., Hilyard, D., Hilyard, D.F., Horn, E., Jern, N., Kanto, D., Keane, M.J., Kibrick, R.I., Lewis, J.W., Osborne, J., Pardeilhan, G.H., Pfister, T., Ricketts, T., Robinson, L.B., Stover, R.J., Tucker, D., Ward, J., & Wei, M.Z. 1994, *S.P.I.E.*, 2198, 362

Witt, A.N., & Johnson, M.W. 1973, *ApJ*, 181, 363

Zsargo, J., Federman, S.R., & Cardelli, J.A. 1997, *ApJ*, 474, 820

Table 1. Rest Equivalent Widths and Column Densities

Transition	λ (Å)	f^a	S/N	$W_\lambda \pm 1\sigma$ (mÅ)	$N_{\text{linear}}^b \pm 1\sigma$ (cm $^{-2}$)	N_{model}^c (cm $^{-2}$)
Fe II $\lambda 1611$	1611.2005	0.00102	26	27.9 ± 3.9	$(1.19 \pm 0.17) \times 10^{15}$	1.23×10^{15}
Si II $\lambda 1808$	1808.0126	0.005527	19	153.5 ± 7.6	$(9.60 \pm 0.48) \times 10^{14}$	1.06×10^{15}
Ni II $\lambda 1455$	1454.8420	0.05954	17	44.6 ± 5.5	$(4.00 \pm 0.49) \times 10^{13}$	3.30×10^{13}
Ni II $\lambda 1317$	1317.2170	0.1458	6	83 ± 15	$(3.71 \pm 0.67) \times 10^{13}$	"
Ni II $\lambda 1370$	1370.1320	0.1309	9	92 ± 12	$(4.23 \pm 0.55) \times 10^{13}$	"
Ni II $\lambda 1710$	1709.6000	0.06884	25	58.7 ± 4.7	$(3.30 \pm 0.26) \times 10^{13}$	"
Ni II $\lambda 1742$	1741.5490	0.1035	24	84.5 ± 5.1	$(3.04 \pm 0.18) \times 10^{13}$	"
Ni II $\lambda 1752$	1751.9100	0.06380	26	65.5 ± 4.8	$(3.78 \pm 0.28) \times 10^{13}$	"
C I $\lambda 1657$	1656.9283	0.1405	25	29.2 ± 2.4	$(0.855 \pm 0.070) \times 10^{13}$	1.41×10^{13}
C I $\lambda 1560$	1560.3092	0.08041	23	22.1 ± 3.1	$(1.28 \pm 0.18) \times 10^{13}$	"
C II* $\lambda 1336$	1335.7077	0.1149	7	92 ± 12	$(5.07 \pm 0.66) \times 10^{13}$	1.10×10^{14}

^aOscillator strengths (f) from Morton 1991 except for FeII $\lambda 1611$ f -value taken from Cardelli & Savage 1995

^bColumn densities assuming linear curve-of-growth, $N_{\text{linear}} = (1.1296 \times 10^{17})W_\lambda\lambda^{-2}f^{-1}$ cm $^{-2}$

^cVoigt profile model column densities: Fe II and Ni II values result from a 3-cloud sum, C I value includes only a single velocity component

Table 2. Three-Component Voigt Absorption Model

Ion	$\log(N_1)$ ^a	$\log(N_2)$ ^b	$\log(N_3)$ ^c
C I	...	13.15	...
Fe II	14.58	14.75	14.47
Ni II	13.15	13.00	12.95
Si II	14.58	14.65	14.37
C II*	13.29	13.90	13.05

^a $v_1 = -19$ km/s, $b_1 = 15$ km/s

^b $v_2 = 0$ km/s, $b_2 = 2.5$ km/s

^c $v_3 = +12$ km/s, $b_3 = 10$ km/s

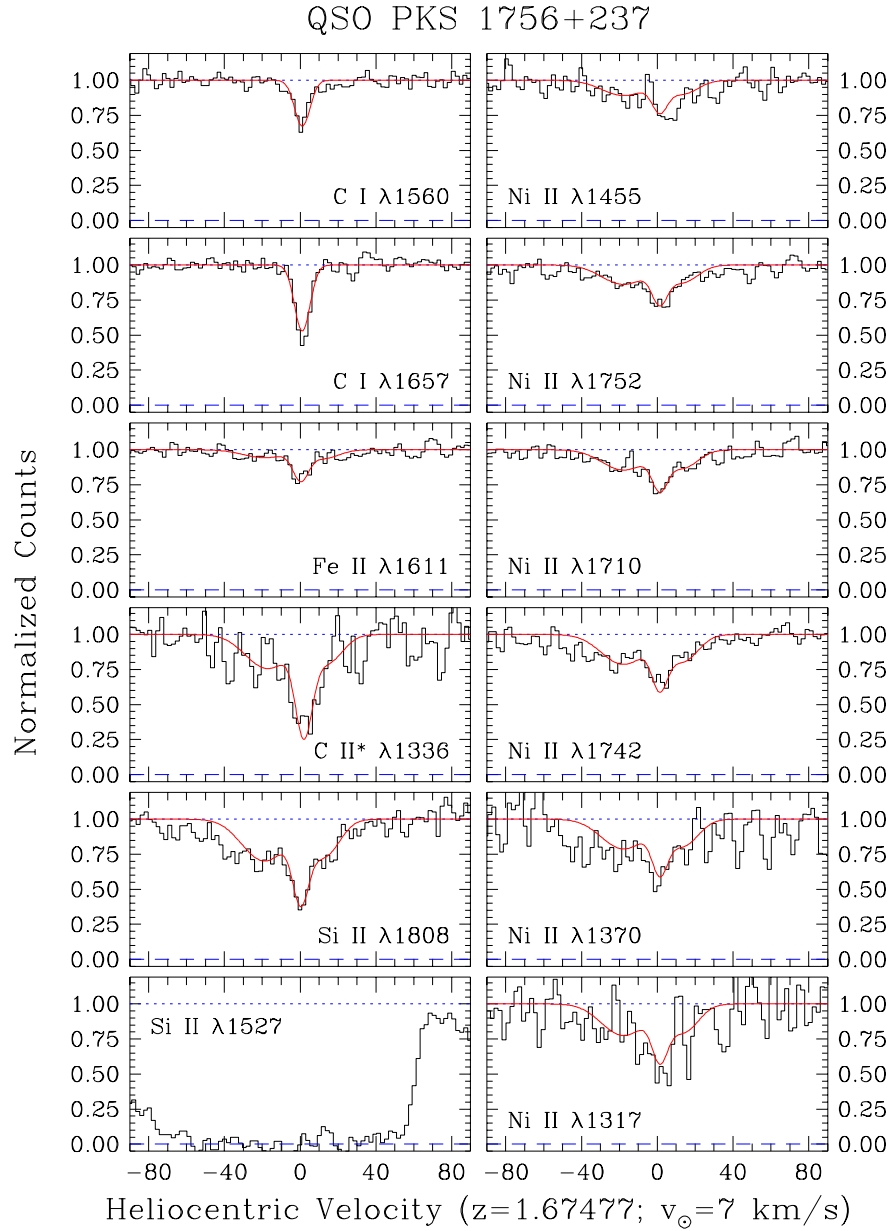


Fig. 1.— Weak Ni II, Fe II, C I* and C I features along with saturated Si II $\lambda 1527$ in the $z = 1.6748$ absorption system toward PKS 1756+237. The spectra have been normalized and the observed air wavelengths have been converted to vacuum heliocentric velocities, with $v = 0$ km s^{-1} corresponding to $z = 1.67477$. Superimposed are Voigt model line profiles.

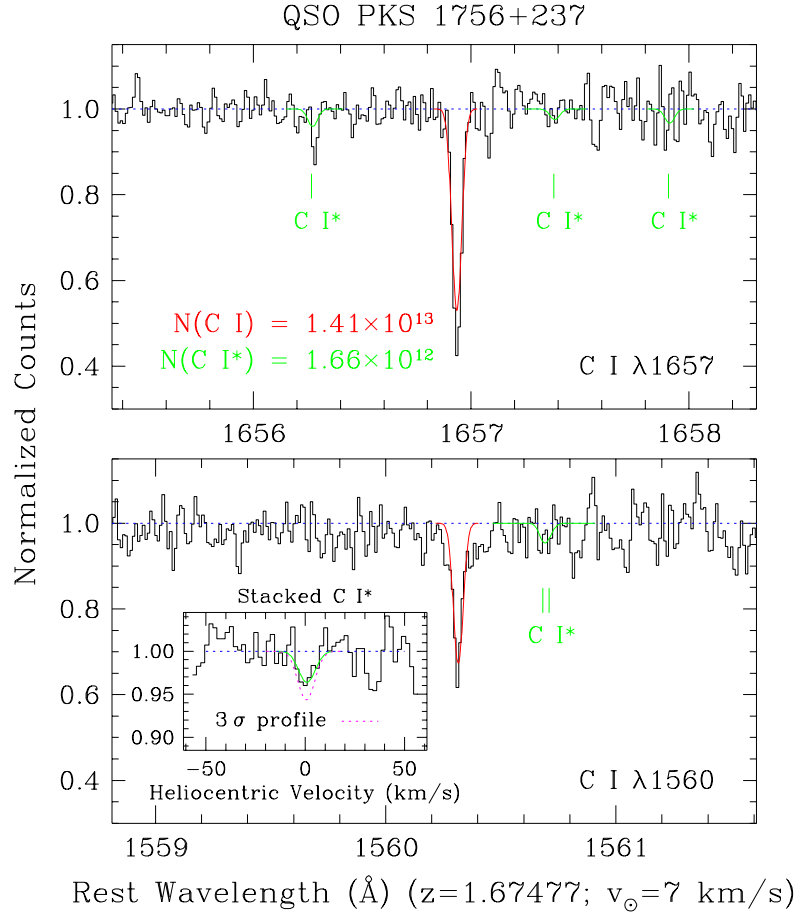


Fig. 2.— C I $\lambda 1657$ (top panel) and $\lambda 1560$ (bottom panel) ground-state lines at $z = 1.67477$ toward PKS 1756+237. Superimposed on each line is our adopted model profile. Also plotted are the expected strengths for the four excited-state C I* lines with the redshifted CMBR as the only source of C I excitation. In the inset figure (bottom panel) the four C I* lines have been shifted to a common heliocentric velocity scale and averaged. Similarly, the expected C I* profile and our 3σ upper-limit have been stacked and superimposed.

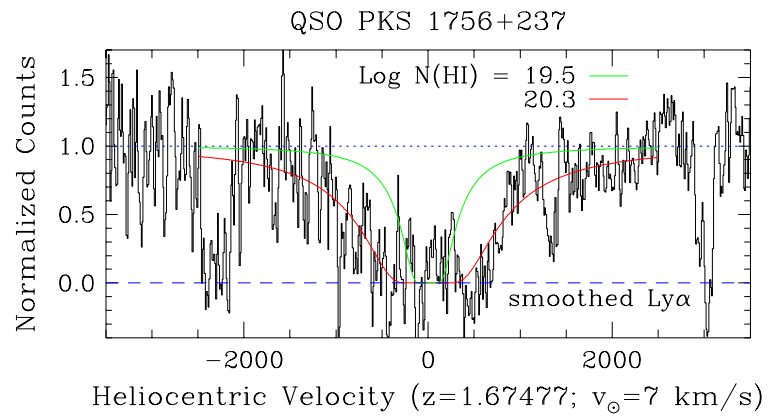


Fig. 3.— Ly α absorption at $z = 1.67477$ toward PKS 1756+237. The data have been smoothed over 11 pixels and rebinned to a dispersion of 10 km/s. Superimposed on the bottom panel are $N(\text{HI}) = 3.16 \times 10^{19}$ and 2.0×10^{20} cm $^{-2}$ Voigt profiles with the same b -value and velocity found from the C I lines.